APPLIED GEOPHYSICS, Vol.13, No.1 (March 2016), P. 127-134, 6 Figures.
DOI:10.1007/s11770-016-0545-1

Improved random noise attenuation using *f–x* empirical mode decomposition and local similarity*

Gan Shu-Wei[1], Wang Shou-Dong♦[1], Chen Yang-Kang[2], Chen Jiang-Long[1], Zhong Wei[1], and Zhang Cheng-Lin[1]

Abstract: Conventional *f–x* empirical mode decomposition (EMD) is an effective random noise attenuation method for use with seismic profiles mainly containing horizontal events. However, when a seismic event is not horizontal, the use of *f–x* EMD is harmful to most useful signals. Based on the framework of *f–x* EMD, this study proposes an improved denoising approach that retrieves lost useful signals by detecting effective signal points in a noise section using local similarity and then designing a weighting operator for retrieving signals. Compared with conventional *f–x* EMD, *f–x* predictive filtering, and *f–x* empirical mode decomposition predictive filtering, the new approach can preserve more useful signals and obtain a relatively cleaner denoised image. Synthetic and field data examples are shown as test performances of the proposed approach, thereby verifying the effectiveness of this method.
Keywords: Random noise attenuation, *f–x* empirical mode decomposition, local similarity, dipping event

Introduction

Random noise attenuation plays an important role in modern seismic data processing (Chen et al., 2015; Qu et al., 2015; Yang et al., 2015), and this has particularly been the case since the popularization of the simultaneous-source acquisition technique (Chen et al., 2014a, 2014b; Chen, 2014). Although *f–x* empirical mode decomposition (EMD) is effective for NMO-corrected and post-stack horizontal events (Bekara and van der Baan, 2009), it cannot effectively remove random noise when the subsurface structure becomes complex. This inability is related to a serious dipping-signal-loss problem from the removal of most dipping events within seismic data.

To ameliorate this problem, Chen et al. (2012) and Dong et al. (2013) used wavelet and curvelet transforms, respectively, to select and retrieve useful signals from a noise section. In addition, Chen and Ma (2014) proposed the prediction of a useful signal in a noise section after *f–x* EMD via *f–x* empirical mode decomposition predictive filtering (EMDPF). The problem of these approaches significantly decreases the signal-to-noise (SNR) of the finally denoised section because these approaches will also retrieve a certain amount of noise

Manuscript received by the Editor February 12, 2015; revised manuscript received March 12, 2016.
*This research is supported by the National Natural Science Foundation of China (No. 41274137) and the National Engineering Laboratory of Offshore Oil Exploration.
1. China University of Petroleum (Beijing), Beijing 102200, China.
2. The University of Texas at Austin, Austin TX, USA.
3. Research Institute of West-South Oil Company, PetroChina, Chengdu 610051, China.
♦Corresponding author: Wang Shou-Dong (Email: ctlab@cup.edu.cn)

when extracting effective signals. Chen et al. (2014c) presented an overview of all EMD-based approaches used in random noise attenuation.

In this study, we aim to retrieve useful signals according to local similarity that are evident between a noise section after *f–x* EMD and a denoised section after *f–x* predictive filtering. In this respect, a weighting operator is designed to select a signal point that has a high local similarity in a noise section. The benefit of this approach is that we can retrieve a small number of useful signals without significantly altering the SNR from an f–x EMD denoised section. In addition, synthetic data and two field datasets demonstrate that this approach yields enhanced denoising performance.

Theory and methodology

f–x EMD

f–x EMD was proposed by Bekara and van der Baan (2009) to attenuate random noise. EMD is useful in the time–frequency analysis of nonlinear and nonstationary signals, where any complicated signal can be decomposed to a finite set of intrinsic mode functions (IMFs) using EMD. IMFs are constructed to satisfy two conditions: (1) The number of extrema and zero crossings must be equal to each other, or differ by one at the most; and (2) at any point the mean value of the envelope defined by the local maxima and the envelope defined by the local minima must be zero. The advantage of IMFs is able to capture the nonstationary and nonlinear information from the signals, and the IMFs are approximately orthogonal to each other.

Bekara and van der Baan (2009) applied EMD to each frequency slice within the *f–x* domain and removed the first IMF, which mainly represented higher wavenumber components, e.g., random noise. Their methodology can be summarized as

$$\hat{\mathbf{s}}(m,t) = \mathcal{F}^{-1}\left(\sum_{n=2}^{N} \mathbf{C}_n(m,w)\right), \tag{1}$$

$$\mathcal{F}\mathrm{d}(m,t) = \sum_{n=1}^{N} \mathbf{C}_n(m,w), \tag{2}$$

where $\hat{\mathbf{s}}(m,t)$ and $\mathbf{d}(m, t)$ denote the estimated signal and acquired noisy signal; $\mathcal{F}$ and $\mathcal{F}^{-1}$ denote the forward and inverse Fourier transform along the time axis, respectively; $\mathbf{C}_n$ denotes the nth EMD decomposed component; and w denotes frequency.

The detailed algorithm steps used for *f–x* EMD (Bekara and van der Baan, 2009) are shown as follows:

(1) To hasten the decomposition process, empirically select a time window (500 × 500) and transform the data to the *f–x* domain.

(2) For every frequency:

(a) Separate the real and imaginary parts within the spatial sequence,

(b) Compute the first IMF for the real signal and subtract the first IMF to obtain the filtered real signal,

(c) Repeat (a) and (b) for the imaginary part,

(d) Combine to create the filtered complex signal.

(3) Transform data back to the *t–x* domain.

(4) Repeat (3) and (4) for the following time window.

Signal retrieval using local similarity

Local similarity was originally defined by Fomel (2007a) and is one of the most useful local seismic attributes; it measures local seismic signal characteristics in the neighborhood at various points. Local similarity has been successfully applied in different areas of seismic data processing, such as multi-component image registration (Fomel, 2007a), time-lapse registration (Fomel and Jin, 2009; Zhang et al., 2013), and time–frequency analysis (Liu et al., 2011). To measure the local similarity between two signals, Fomel defined the local similarity of vector **a** and **b** as

$$\mathbf{c} = \sqrt{\mathbf{c}_1^T \mathbf{c}_2},$$

where $\mathbf{c}_1$ and $\mathbf{c}_2$ are obtained from two least squares minimization problem,

$$\mathbf{c}_1 = \arg\min_{\mathbf{c}_1} \left\| \mathbf{a} - \mathbf{C}_1 \mathbf{b} \right\|_2^2, \tag{3}$$

$$\mathbf{c}_2 = \arg\min_{\mathbf{c}_2} \left\| \mathbf{b} - \mathbf{C}_2 \mathbf{a} \right\|_2^2, \tag{4}$$

where $\mathbf{C}_i$ is a diagonal operator composed from elements of $\mathbf{c}_i$: $\mathbf{C}_i = diag(\mathbf{c}_i)$, $i = 1, 2$. The least-squares problems (3) and (4) can be solved with the help of shaping regularization (Fomel, 2007b) using a local smoothness constraint,

$$\mathbf{c}_1 = \left[\lambda^2 \mathbf{I} + \mathbf{S}\left(\mathbf{A}^T\mathbf{A} - \lambda^2\mathbf{I}\right)\right]^{-1} \mathbf{S}\mathbf{A}^T\mathbf{b}, \tag{5}$$

$$\mathbf{c}_2 = \left[\lambda^2 \mathbf{I} + \mathbf{S}\left(\mathbf{B}^T\mathbf{B} - \lambda^2\mathbf{I}\right)\right]^{-1} \mathbf{S}\mathbf{B}^T\mathbf{a}, \tag{6}$$

where **A** is a diagonal operator composed from the elements of **a**: $\mathbf{A} = diag(\mathbf{a})$, **B** is a diagonal operator composed from the elements of **b**: $\mathbf{B} = diag(\mathbf{b})$, **S** is a smoothing operator, and λ is a parameter controlling the physical dimensionality that enables fast convergence when inversion is implemented iteratively.

The principle of using local similarity to retrieve a signal is based on the assumption that the noise section after *f–x* EMD, and the denoised section after *f–x* predictive filtering, should have low local similarity. A weighting operator can be designed to retrieve the useful signal from the EMD-based noise section as,

$$W(t,x)=\begin{cases}1 & for\, V_{n,s}(t\ x)>v_2,\\ \dfrac{V_{n,s}(t,x)-v_1}{v_2-v_1} & for\, v_1\le V_{n,s}(t\ x)\le v_2,\\ 0 & for\, V_{n,s}(t\ x)<v_1\end{cases} \quad (7)$$

where v_1 and v_2 define two thresholds, and $V_{n,s}(t, x)$ denotes the local similarity of the noise section to the denoised section. Generally, when the similarity is relatively high (for example greater than 0.4) the components in the noisy section will all be useful signals. However, if the similarity is rather low, the components in the noisy section will consist completely of noise. When the similarity is in between these extremes, the components will consist of a combination of useful signals and noise. In this study, we use a linear weighted method to obtain useful signals. In the three examples below, we choose v_1 and v_2 as 0.2 and 0.4, respectively.

Combining the *f–x* EMD and signal retrieving approach using local similarity, we propose the following improved random noise attenuation algorithm following the basic framework of *f–x* EMD by:

1. Denoising using *f–x* EMD and obtaining corresponding denoised and noise sections.
2. Denoising using *f–x* predictive filtering and obtaining a corresponding denoised section.
3. Computing the local similarity between the noise section after *f–x* EMD and the denoised section after conducting *f–x* predictive filtering.
4. Applying a weighting operator, as defined in equation 7, to the *f–x* EMD-based noise section to obtain a section of the retrieved signal.
5. Summing the denoised section after *f–x* EMD and the retrieved signal to form the output.

It is important to stress that during the process of calculating the local similarity between two signals, the *f–x* predictive filtering acts as a filter that roughly estimates the useful signal. However, the ability to achieve this is not restricted to use of the *f–x* predictive filtering, and can be obtained using other commonly used denoising filters.

Synthetic and field data examples

Synthetic data example

Figure 1 is a synthetic single-shot seismic dataset composed of two horizontal events and one dipping event (Figure 1a shows data without noise and Figure 1b shows added background white noise). To make a

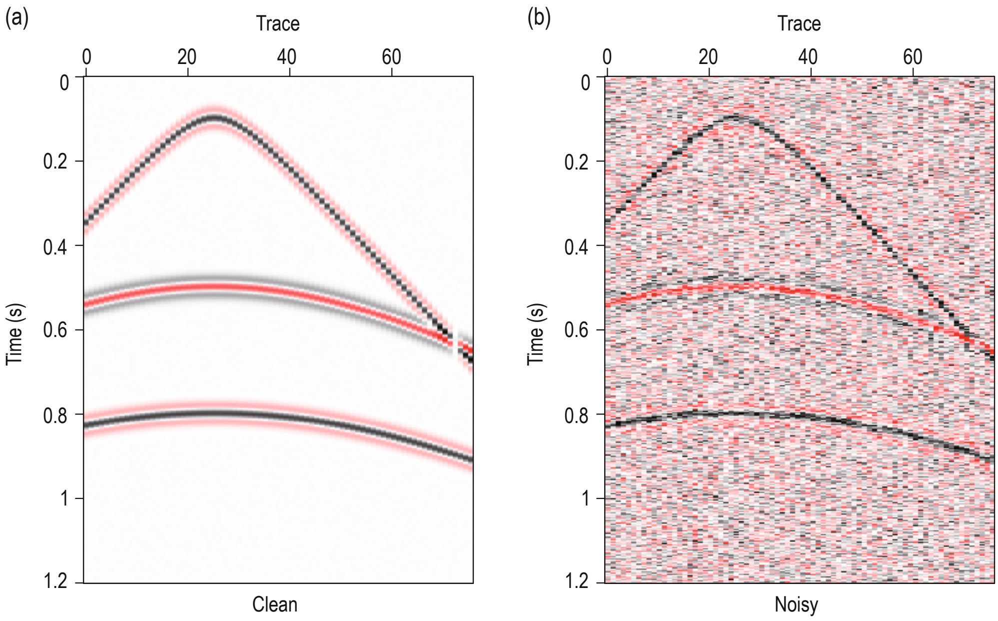

Fig.1 (a) Clean synthetic dataset; (b) Noisy synthetic dataset.

comparison between the denoising effects of the various approaches, we apply *f–x* EMD, *f–x* deconvolution, and the approach proposed in this paper to the noisy dataset. We can therefore conclude from Figure 2a and 2d that the *f–x* EMD is quite effective in denoising the section composed of horizontal events. However, it also causes a considerable loss of energy during the dipping events and thus cannot be applied to complicated profiles. The denoising result using the *f–x* deconvolution is shown in Figure 2b, and Figure 2e shows the corresponding noise section. We can see from the noise section that while the background white noise is greatly attenuated, the useful signal is also evidently attenuated, and this is not desirable because of the decreased resolution. The denoising result of our proposed approach is shown in Figure 2c and its corresponding noise section is shown in Figure 2f. It is evident from these figures that this approach can effectively protect the energy of the dipping events, and compared with *f–x* deconvolution the three events are well displayed in the denoised section, the noise section is well distributed, and minimal useful energy is lost.

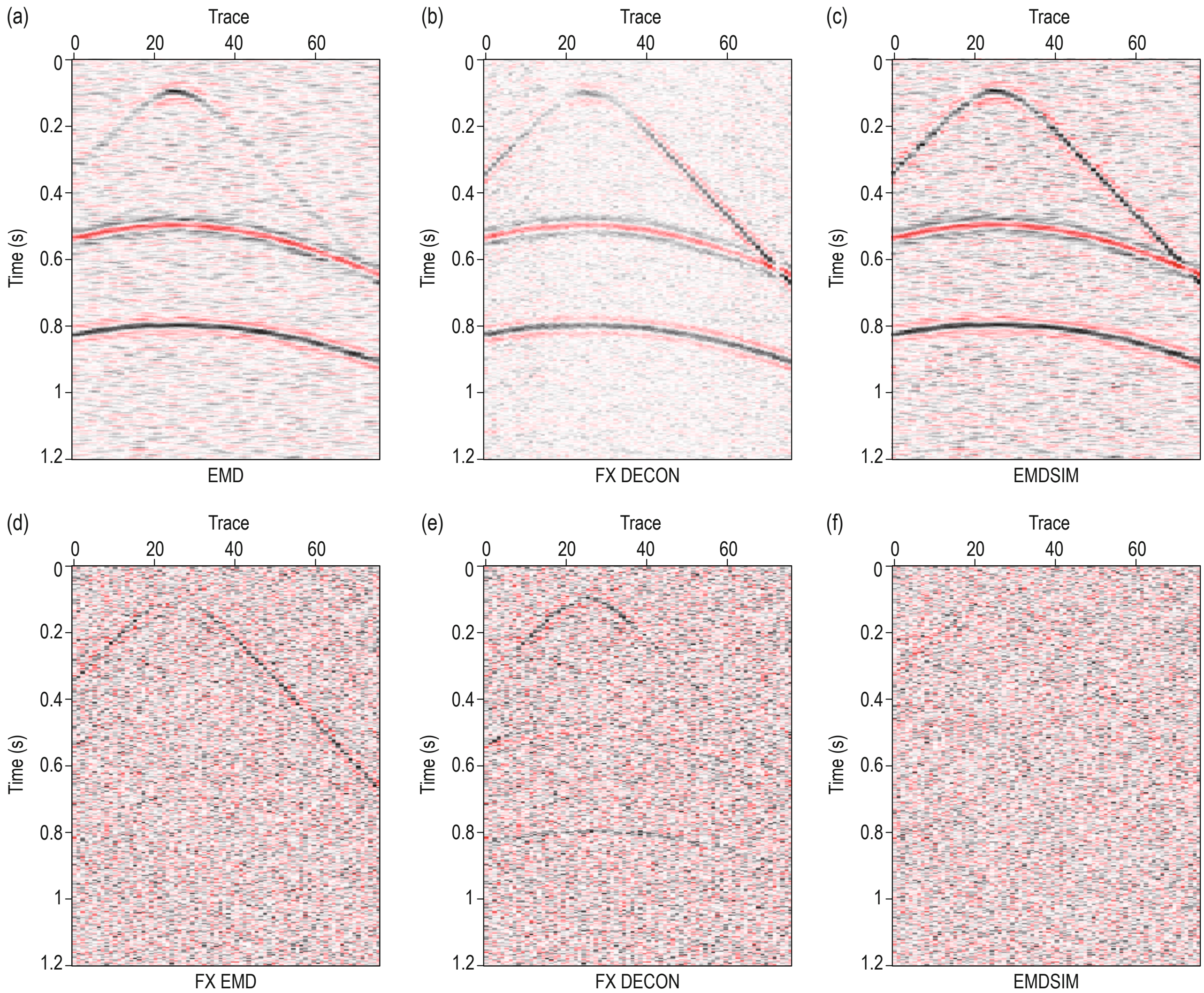

Fig.2 Denoising performance comparison.

(a) Denoised using *f–x* EMD; (b) denoised using *f–x* deconvolution; (c) denoised using the proposed approach; (d) noise section corresponding to (a); (e) noise section corresponding to (b); (f) noise section corresponding to (d).

Field data examples

In order to compare the proposed approach with the traditional *f–x* EMD approach, we further apply these two approaches to land field data. Figure 3a shows the noisy post-stack land field data after normal-moveout correction (Chen et al., 2014b). The traditional *f–x* EMD and the proposed improved EMD are then used to attenuate random noise to this profile, respectively.

Figure 4a shows the denoised section using *f–x* EMD, and the corresponding noise section is shown in Figure 4b. The denoised results using the proposed approach are shown in Figure 4c, and Figure 4d shows the corresponding noise section. As the seismic profile is mainly composed of horizontal events, a comparison of these two denoised sections shows that the denoised section using the proposed approach is as clean as that of *f–x* EMD. However, *f–x* EMD harms many of the dipping events, as shown by a comparison of signal preservation shown in the frame boxes in Figure 4.

To further verify the performance, we use a seismic profile from the South China Sea that consists of more complicated underground strata (Chen and Ma, 2014), where the noisy post-stack data are shown in Figure 3b. To enable this we select four different approaches

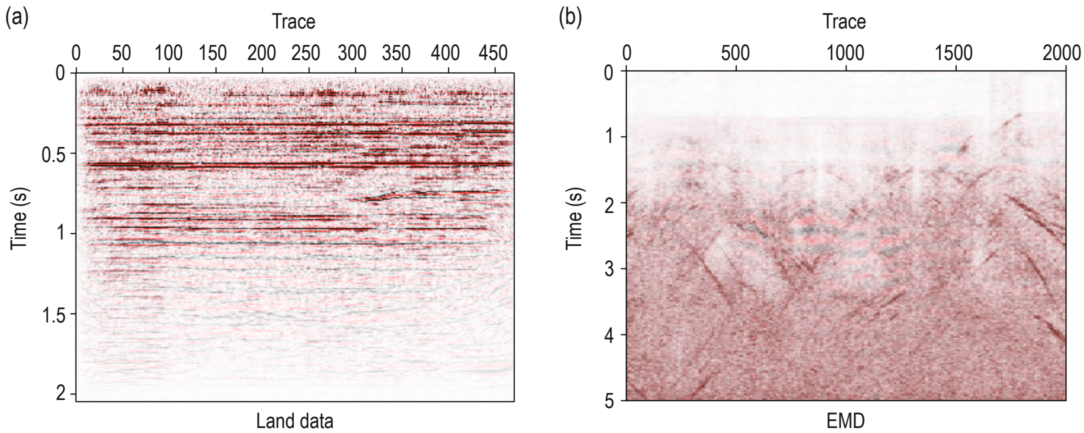

Fig.3 (a) Land field data example; (b) South China Sea field data example.

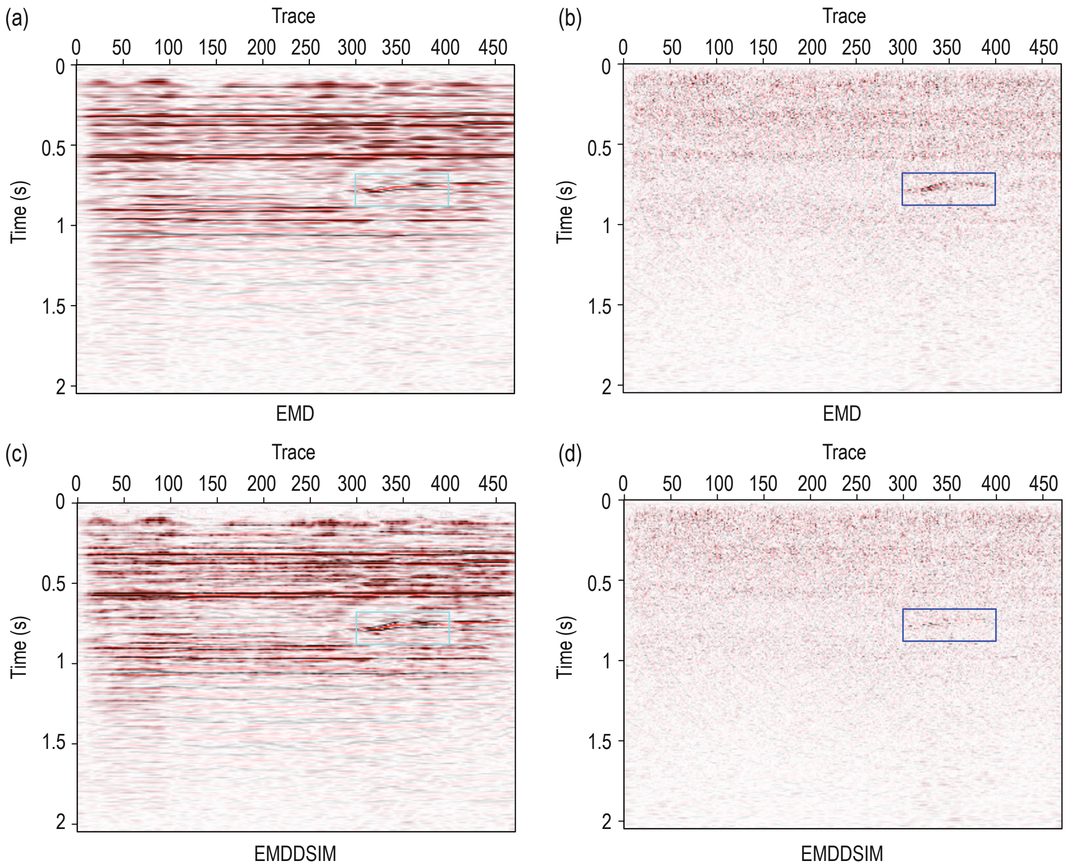

Fig.4 Comparison of denoising performance.
(a) Denoising using *f–x* EMD; (b) noise section corresponding to (a); (c) denoising using proposed approach; (d) noise section corresponding to (c).

to attenuate random noise. Figure 5a presents the denoised section using *f–x* EMD and its corresponding noise section is shown in Figure 5b. Although this approach can attenuate most of the background noise, the noise section also contains a lot of useful signals because the strata are composed of many dipping events. The denoised result of *f–x* predictive filtering and its corresponding noise section are shown in Figure 5c and 5d, respectively. However, in order to protect the dipping events this approach has a tradeoff in that more useful energy is preserved while the denoised performance is not well satisfied. Figure 5e shows the denoised result using *f–x* EMDPF, and Figure 5f shows the corresponding noise section; part of the dipping events signal is retrieved when applying the predictive filter to the first intrinsic mode function. However, there is no evident energy loss in the noise section (as shown in Figure 5b), but as the predictive filter also returns part of the background noise while retrieving the useful signal the denoised performance is also not ideal. The last approach used is that of the proposed improved EMD, and the denoised result and corresponding noise section are shown in Figures 5g and 5h, respectively. It is evident that the denoised section

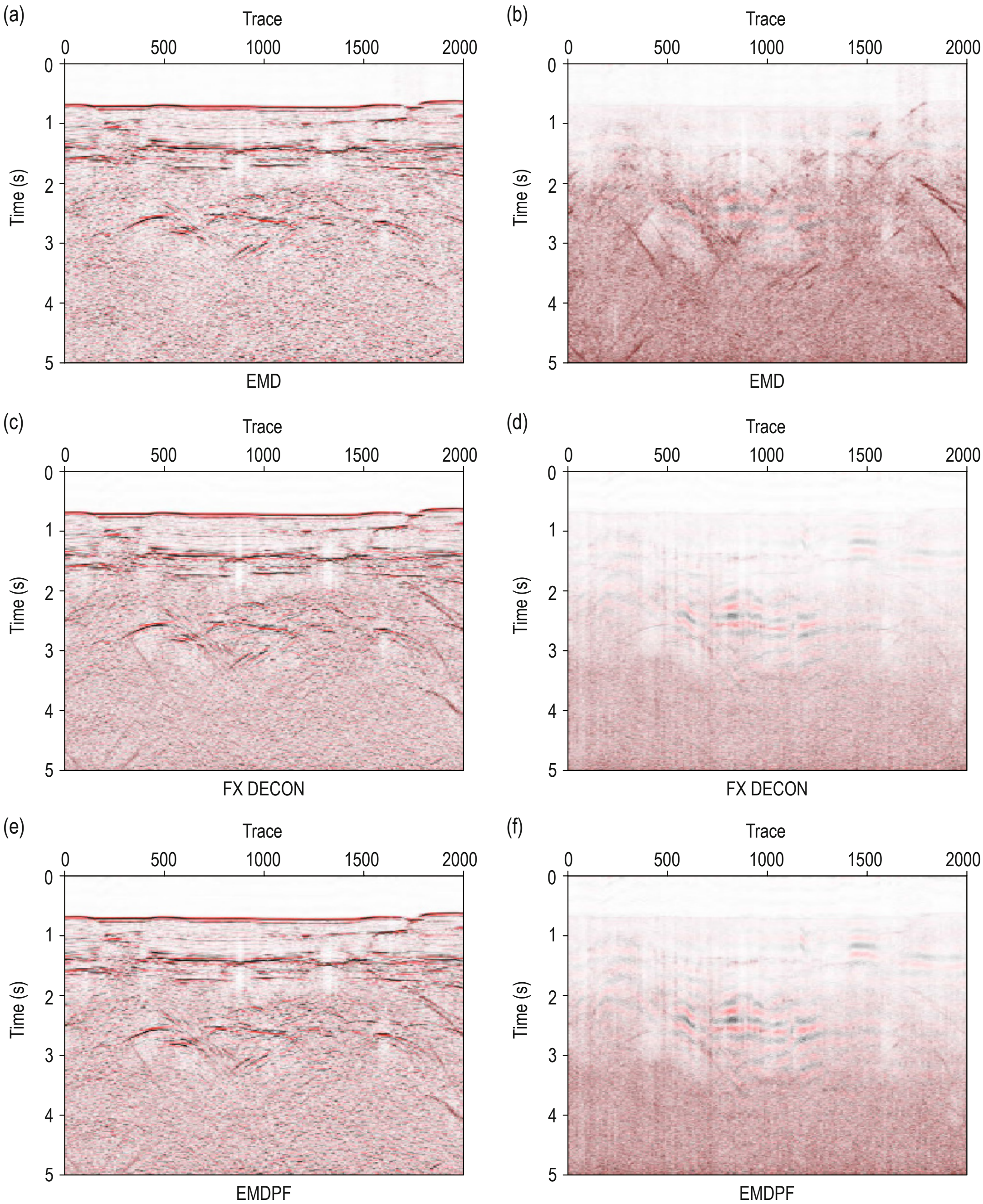

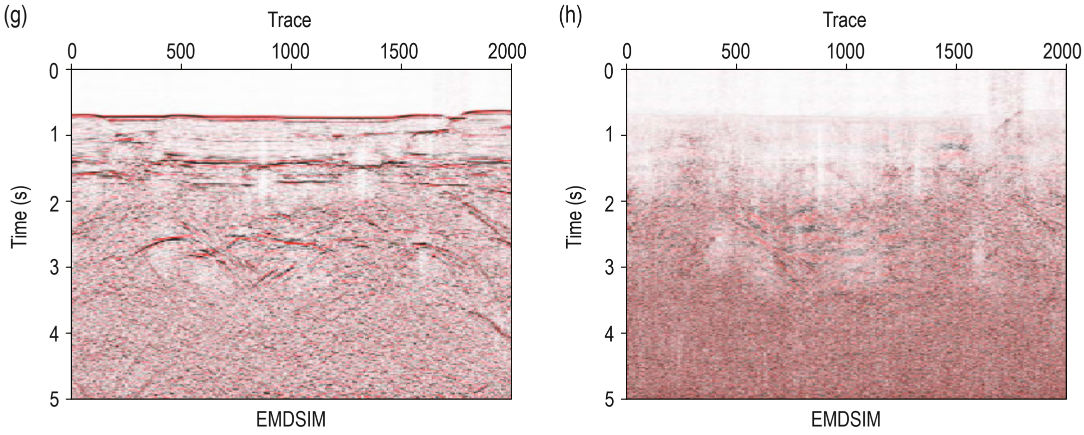

Fig.5 Comparison of denoising performance.

(a) Denoising using *f–x* EMD; (b) noise section corresponding to (a); (c) denoising using *f–x* predictive filtering; (d) noise section corresponding to (c); (e) denoising using *f–x* EMDPF; (f) noise section corresponding to (e); (g) denoising using the proposed approach; (h) noise section corresponding to (g).

is much cleaner using the proposed approach than when using *f–x* predictive filtering or *f–x* EMDPF; it is a much more effective approach for retrieving useful signals using local similarity than using the predictive filter and the denoised section has a much higher SNR. Figure 6 shows the retrieved section using a weighted local similarity operator. The principle of our denoising method is based on signal retrieving from the noise section and it therefore inevitably returns part of the noise. However, it is not possible to ascertain whether or not too much noise has been retrieved from the results of the final overall denoising effect.

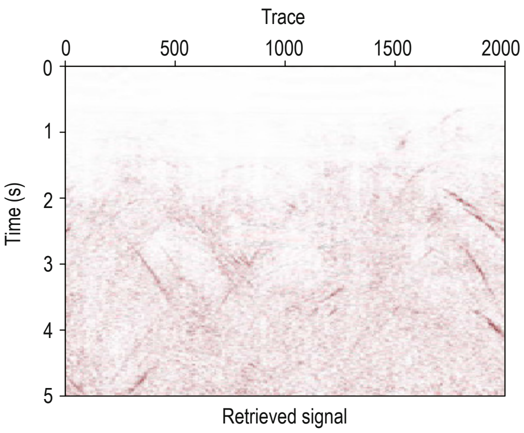

Fig.6 Retrieved section from South China Sea profile using weighted local similarity operator.

Conclusions

We propose an improved approach for random noise attenuation using *f–x* EMD. The basic idea of the new approach is to retrieve useful signals in the noise section for use with conventional *f–x* EMD, according to local similarities between the *f–x* EMD-based noise section and the *f–x* predictive based denoised section. Synthetic data and field data examples show that *f–x* EMD is able to preserve the horizontal events and leave a small number of useful dipping signals in the noise section, which can be identified from similarities. Results therefore show the proposed approach is able to obtain an enhanced denoising performance.

References

Bekara, M. and van der Baan M., 2009, Random and coherent noise attenuation by empirical mode decomposition: Geophysics, **74**(5), V89–V98.

Chen, W., Wang, S., Zhang, Z., and Chuai, X., 2012, Noise reduction based on wavelet threshold filtering and ensemble empirical mode decomposition: 82nd Annual International Meeting, SEG, Expanded Abstracts, 1–6.

Chen, Y., 2014, Deblending using a space-varying median filter: Exploration Geophysics, 82−87.

Chen, Y., Fomel, S., and Hu, J., 2014a, Iterative deblending of simultaneous-source seismic data using seislet-domain shaping regularization: Geophysics, **79**(5), V179–V189.

Chen, Y., Gan, S., Liu, T., Yuan, J., Zhang, Y., and Jin, Z., 2015, Random noise attenuation by a selective hybrid approach using *f–x* empirical mode decomposition: Journal of Geophysics and Engineering, **12**, 12–25.

Chen, Y. and Ma, J., 2014, Random noise attenuation by *f* −*x* empirical mode decomposition predictive filtering:

Geophysics, **79**(3), V81–V91.

Chen, Y., Yuan, J., Jin, Z., Chen, K., and Zhang, L., 2014b, Deblending using normal moveout and median filtering in common-midpoint gathers: Journal of Geophysics and Engineering, **11**(4), 045012.

Chen, Y., Zhou, C., Yuan, J., and Jin, Z., 2014c, Application of empirical mode decomposition to random noise attenuation of seismic data: Journal of Seismic Exploration, **23**(6), 481–495.

Dong, L., Li, Z., and Wang, D., 2013, Curvelet threshold denoising joint withempirical mode decomposition: 83rdAnnual International Meeting, SEG, Expanded Abstracts, 4412–4416.

Fomel, S., 2007a, Local seismic attributes: Geophysics, **72**(3), A29–A33.

Fomel, S., 2007b, Shaping regularization in geophysical-estimation problems: Geophysics, **72**(2), R29–R36.

Fomel, S., and Jin, L., 2009, Time-lapse image registration using the localattributes: Geophysics, **74**(2), A7–A11.

Liu,G., Fomel, S., and Chen, X., 2011, Time-frequency analysis of seismic data using local attributes: Geophysics, **76**(6), P23–P34.

Qu, S., Zhou, H., Chen, Y., Yu, S., Yuan, J., Wang, Y., and Qin, M., 2015, An effective method of reducing harmonic distortion in correlated vibroseis data: Journal of Applied Geophysics, **115**, 120–128.

Yang, W., Wang, R., Chen, Y., Wu, J., Qu, S., Yuan, J., and Gan, S., 2015, Application of spectral decomposition using regularized non-stationary autoregression to random noise attenuation: Journal of Geophysics and Engineering, **12**(2), 175–187.

Zhang, R., Song, X., Fomel, S., Sen, M. K., and Srinivasan, S., 2013, Time-lapse seismic data registration and inversion for CO2 sequestration study at Cranfield: Geophysics, **78**(6), B329–B338.

Gan Shu-Wei is currently a postgraduate student of Geophysical Prospecting at the China University of Petroleum (Beijing). He received a B.S. in Mechanical Engineering at Nanjing University of Aeronautics and Astronautics in 2012. His research area is that of seismic signal processing, which mainly includes seismic data denoising, interpolation, and simultaneous source data deblending.